PLUTO FOLLOWED ITS HEART: TRUE POLAR WANDER OF PLUTO DUE TO THE FORMATION AND EVOLUTION OF SPUTNIK PLANUM. J. T. Keane[1] and I. Matsuyama[1], [1]Lunar and Planetary Laboratory, Department of Planetary Science, University of Arizona, Tucson, AZ, 85721, USA (jkeane@lpl.arizona.edu).

Overview: The geographic location of Sputnik Planum (the large, N_2 ice filled, convecting "heart" of Pluto [1]) is suspiciously close to the tidal axis of Pluto (Fig. 1). If Sputnik Planum (SP) were a large positive mass anomaly—perhaps due to loading of N_2 ice—then SP would naturally migrate to the tidal axis as Pluto approaches a minimum energy state. In this work, we investigate the feasibility of reorientation (i.e. true polar wander) of Pluto by Sputnik Planum, and its implications for Pluto's interior structure, global tectonic patterns, and volatile cycling.

Reorientation due to Sputnik Planum: SP is a large, ~20° radius, ~4 km deep, probable impact basin [2] located near the anti-Charon point, at 176°E, 24°N. This location, near the anti-Charon point, is consistent with SP being a positive mass anomaly, which resulted in true polar wander (TPW) of Pluto, placing it near the tidal axis in order to minimize rotational and potential energy. There is only a 10% probability of placing an anomaly this close to a tidal axis by chance.

On other solar system bodies, the formation and evolution of a large impact basin can easily produce positive, neutral (i.e. compensated), or negative mass anomalies that result in TPW [3-5]. For this preliminary work, we assume that the underlying basin is predominantly compensated, and instead focus on reorientation due to the subsequent infill of several kilometers of N_2 ice [6-7].

The ability of any mass anomaly to reorient a body is counteracted by the planet's elastic lithosphere, which may preserve an earlier rotational or tidal bulge. At present, no bulge (fossil or otherwise) has been detected at Pluto [1]. We assume that Pluto has a rigid fossil figure, formed in its present spin/orbit configuration with Charon, consistent with the upper limit of Pluto's oblateness [1]. Under this assumption, we determined the possible initial formation locations of SP, as a function of the thickness of N_2 ice within the basin (Fig. 2). If the underlying basin is not compensated, then these thicknesses are lower limits if it is a negative anomaly, and upper limits if it is a positive anomaly. Similarly, the degree of differentiation, strength of the lithosphere, magnitude of fossil bulge, and presence of an ocean can modulate these results (although the general patterns in Fig. 2 will remain the same). In this work, we assume a nominal Pluto interior structure; with a 250 km thick ice crust, with elastic thickness of 50 km, overlying an ocean. Nonetheless, the non-zero latitude of SP places interesting constraints on the initial location of SP, and any subsequent reorientation. *Not just any mass anomaly will reorient Pluto to place SP at its present location. SP likely formed at higher latitude, either at 90°E or 180°E.*

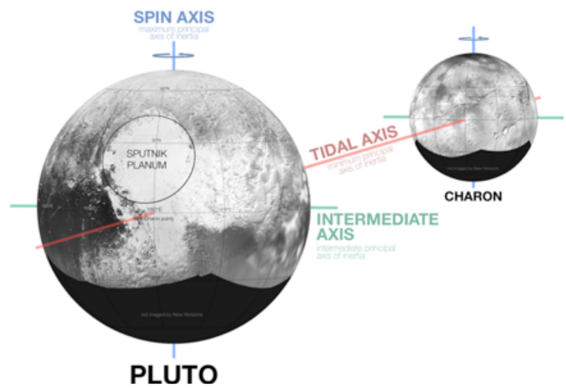

Fig. 1: *The location of Sputnik Planum with respect to Pluto's principal axes of inertia. Pluto/Charon maps: NASA/JHUAPL/SwRI.*

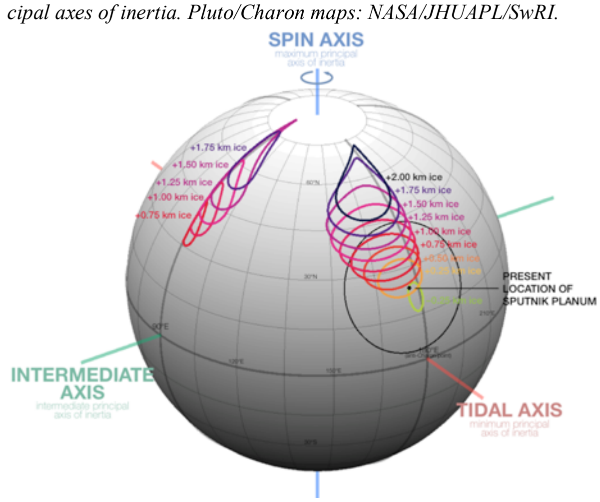

Fig. 2: *Contours enclose regions where you could place a mass sheet the size of Sputnik Planum, with the listed equivalent thickness of N_2 ice, and reorient Pluto to place Sputnik Planum to within 5° of its present location. Note that ice sheet thicknesses required for true polar wander are consistent with estimates for the thickness of N_2 ice in Sputnik Planum [6-7].*

Tectonic Stresses due to True Polar Wander: Reorientation of a planet generates stresses in the lithosphere, which can result in characteristic global tectonic patterns [8-9]. Pluto indeed shows a global, nonrandom system of extensional faults and graben (Fig. 3a-b) [1]. The lack of obvious thrust or strike-slip faulting likely reflects global extensional stresses associated with the freezing of a subsurface ocean, and the resulting expansion of Pluto [10]. Using our initial locations of SP (Fig. 2), we calculated tectonic patterns for a range of possible reorientation scenarios (Fig. 3c-

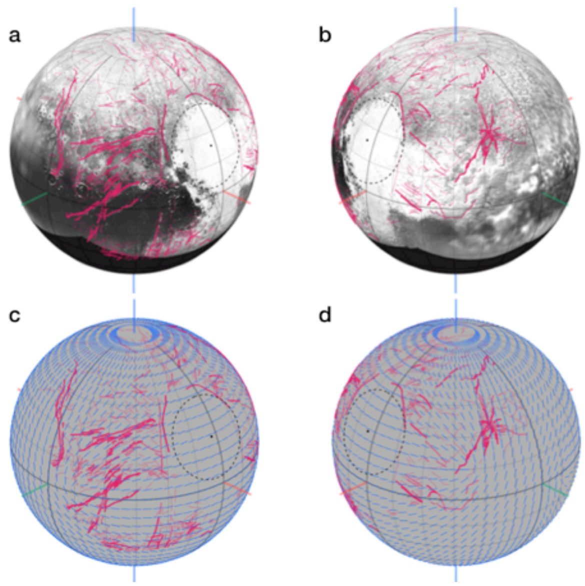

Fig. 3: *Observed (a-b) and modeled (c-d) tectonic patterns on Pluto. Observed tectonic patterns (pink) were mapped using publicly available global maps (NASA/JHUAPL /SwRI). (c-d) show predicted faults for the case of global expansion (resulting in all extensional faults), TPW and mass loading due to Sputnik Planum. We assume a 250 km thick ice shell, with elastic lithosphere thickness of 50 km, overlying a 50 km thick ocean.*

d). While no model matches *all* observed faults, our preferred model is for TPW driven by a positive mass anomaly, coupled with faulting due to loading of SP. Tectonic patterns based on TPW and loading match the observed pattern better than loading alone.

True Polar Wander of Pluto due to migration of volatiles? Pluto's high obliquity (118°) means that Pluto's equator receives more annual insolation than its poles [11-14]. Generally, the sequestration of volatiles at Pluto's equator would act to inhibit polar wander [15]. However, orbital cycling of Pluto's obliquity (and other orbital elements) can result in the cold-trap latitude band cycling up to ±30°N. Additionally, Pluto's lower atmosphere has a positive temperature gradient [16], meaning that SP (a topographic depression) may be an intrinsic cold-trap. We propose that SP started at higher latitude, and was gradually filled with N_2 over obliquity-evolution timescales (~Myr), and migrated towards the equator and tidal pole.

To investigate the feasibility of this hypothesis, we developed a simple cellular automata model for tracking the migration of volatiles over orbital timescales. In this model, Pluto's surface is discretized into latitude/longitude grid cells, each initially covered in 500-meters of N_2 ice. At each time-step in the model, we determine the annual, zonal-mean insolation pattern, and assign each grid cell a probability of sublimation and condensation dependent on the local insolation. Grid cells within SP are assigned a slightly higher probability of condensation, on the assumption that it is a localized cold-trap. SP is initially located further North and West than its present location. We then randomly select *N* grid points, based on the probability of sublimation, and redistribute a fraction of the N_2 ice in those grids to an equal number of grid points randomly selected based on the probability of condensation. Following each time-step, we evaluate the new global inertia tensor due to volatile redistribution, and determine how the planet would reorient, which then changes the insolation pattern in the subsequent time-step. Fig. 4 shows an example output of this model. Over orbital timescales, volatiles migrate from the equatorial cold traps and become sequestered into SP. As SP loads with N_2, it migrates towards the equator and tidal axis, further enhancing its ability to trap volatiles. The final latitude and longitude is set by the efficiency of this process, the total reservoir of mobile volatiles, and Pluto's fossil figure.

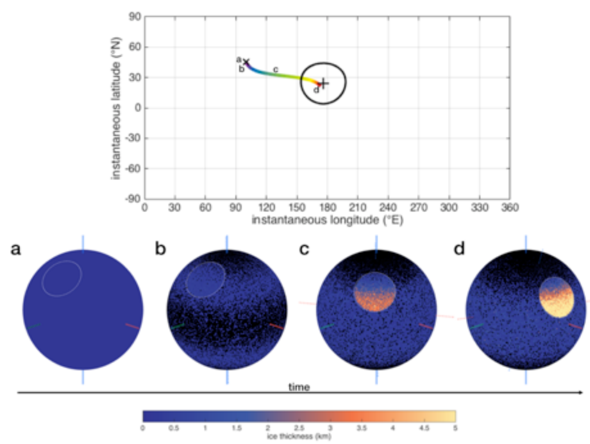

Fig. 4: *Example output of our model for volatile-induced true polar wander of Sputnik Planum. The model starts with a global 500-meter thick N_2 ice layer (a). We assume volatiles migrate to regions of low annual insolation and/or low topography. The N_2 reservoir rapidly migrates into near-equatorial cold trap bands (b-c). However, N_2 ice eventually sequesters into Sputnik Planum (c-d), which is dragged towards the equator and tidal axis. The top panel shows the instantaneous latitude and longitude of Sputnik Planum at each timestep in the model – starting at 90°E, 45°N (a; blue point in top panel) and migrating to its present position 176°E, 24°N (d; red point in top panel).*

References: [1] Stern et al. 2015, Science 350. [2] Schenk et al. 2015, DPS 200.06. [3] Melosh 1975, EPSL 26. [4] Nimmo & Matsuyama 2007, GRL 34. [5] Keane & Matsuyama 2014, GRL 41. [6] Trowbridge et al. 2015, AGU P51D-04. [7] McKinnon et al. 2015, AGU P51A-2041. [8] Melosh 1980, Icarus 44. [9] Matsuyama & Nimmo 2009, JGR 114. [10] Moore et al. 2015, Icarus 246. [11] Dobrovolskis, Peale, & Harris 1997, Pluto and Charon. [12] Hansen, Paige, & Young 2015, Icarus 246. [13] Earle & Binzel 2015, Icarus 250. [14] Hamilton 2015, DPS 200.07. [15] Rubincam 2003, Icarus 163. [16] Hinson et al. AGU P54A-06.